Supplementary Figure 1

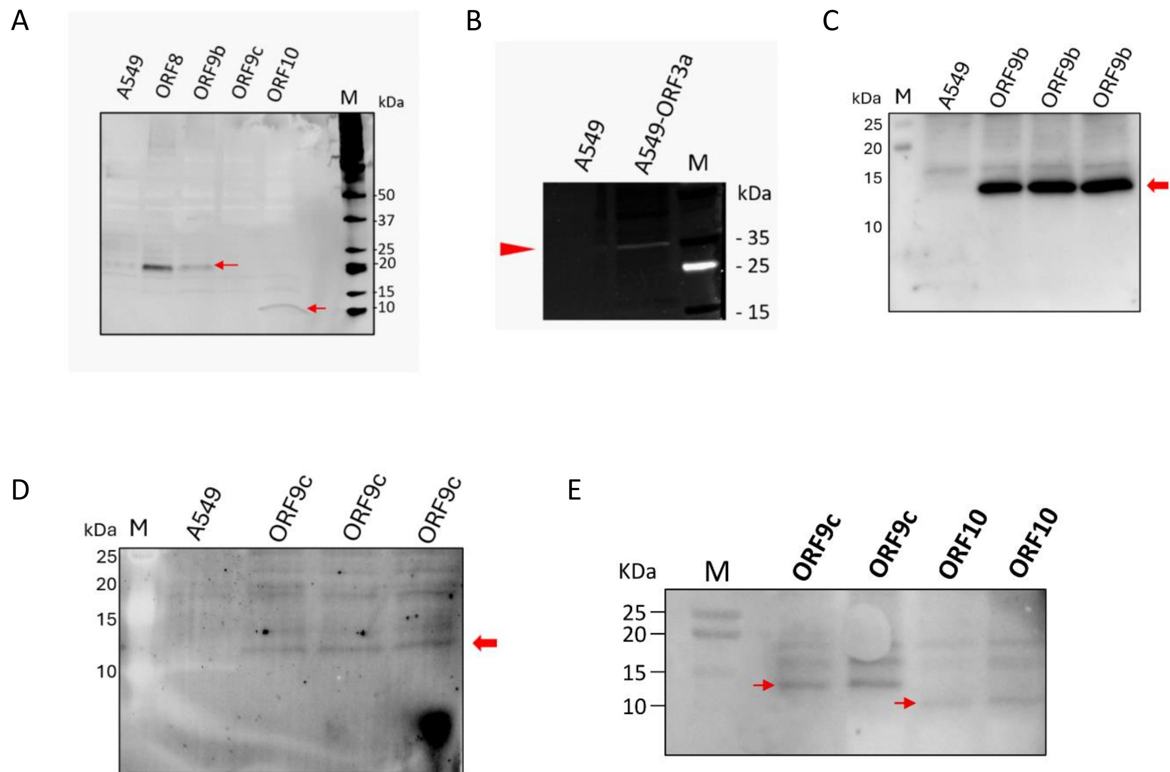

Figure S1. **(A) Detection of ORF9b and ORF10 by Western blot**. Non-transduced (A549) and transduced cells with ORF8, ORF9b, ORF9c and ORF10 whole cell extracts (30 µg) were separated by 4-20% SDS-PAGE and transferred onto a nitrocellulose membrane using Trans-Blot Turbo Transfer System (Bio-Rad) during 7 min at 1.3 A constant (Mixed MW protocol). The membrane was blocking for 1 h in TTBS 5% milk and probing with Strep-Tag Monoclonal Antibody (#SAB2702216, Sigma) overnight at 4ºC. The StarBright Blue 700 Goat anti-mouse IgG antibody (#12004159, Bio-rad) was used to detect the primary antibody. Proteins were visualized by fluorescence using ChemiDoc MP Imaging Systems (Bio-Rad). ORF9b band is shown as a dimer. **(B) Detection of ORF3a by Western blot**. Non-transduced (A549) and transduced cells with ORF3a (A549-ORF3a) whole cell extracts (50 µg) were separated by 4-20% SDS-PAGE and transferred onto a nitrocellulose membrane using Trans-Blot Turbo Transfer System (Bio-Rad) during 30 min at 25 V constant (Standard SD protocol). The membrane was blocking for 1 h in TTBS 5% milk and probing with Strep-Tag Monoclonal Antibody (#SAB2702216, Sigma) overnight at 4ºC. The StarBright Blue 700 Goat anti-mouse IgG antibody (#12004159, Bio-rad) was used to detect the primary antibody. Proteins were visualized by fluorescence using ChemiDoc MP Imaging Systems (Bio-Rad). **(C) Detection of ORF9b by Western blot**. Whole cell extracts from non-transduced A549 cells (40 µg) and increasing amounts of whole cell extracts from ORF9b-transduced cells (30-40-50 µg) were separated by 15% SDS-PAGE and transferred onto a PVDF membrane using Trans-Blot Turbo Transfer System (Bio-Rad) during 7 min at 1.3 A constant (Mixed MW protocol). The membrane was blocking for 1 h in TTBS 5% milk and probing with SARS-CoV-2 ORF9b Monoclonal Antibody (HL1917) (#NBP3-25669, Bio-Techne) overnight at 4°C. The anti-Rabbit IgG (whole molecule)-HRP (#A6154, Sigma) antibody was used to detect the primary antibody. Proteins were visualized by chemiluminiscence using ChemiDoc MP Imaging Systems (Bio-Rad). **(D) Detection of ORF9c by Western blot**. Whole cell extracts from non-transduced A549 cells (50

µg) and increasing amounts of whole cell extracts from ORF9b-transduced cells (50-60-70 µg) were separated by 15% SDS-PAGE and transferred onto a PVDF membrane using Trans-Blot Turbo Transfer System (Bio-Rad) during 7 min at 1.3 A constant (Mixed MW protocol). The membrane was blocking for 1 h in TTBS 5% milk and probing with SARS-CoV-2 ORF9c Monoclonal Antibody (#NBP3-11930, Bio-Techne) overnight at 4°C. The StarBright Blue 700 Goat anti-Rabbit IgG (#12004162, Bio-Rad) antibody was used to detect the primary antibody. Proteins were visualized by fluorescence using ChemiDoc MP Imaging Systems (Bio-Rad). **(E) Detection of ORF9c and ORF10 by Western blot**. Whole cell extracts from cells expressing ORF9c and ORF10 (70 and 90 µg) were separated by 15% SDS-PAGE and transferred onto a PVDF membrane using wet transfer for 10 min at 25 V constant. The membrane was blocked for 1 h at room temperature in TTBS 5% BSA and probed with anti-Strep Tag II Monoclonal Antibody conjugated with biotin (#ABIN962829, Antibodies-online) overnight at 4°C. Pierce® Streptavidin Poly-HRP (#21140, Thermo Scientific) was used to detect the primary antibody for 1 h at room temperature. Proteins were visualized by chemiluminiscence using ChemiDoc MP Imaging Systems (Bio-Rad).

Supplementary Figure 2

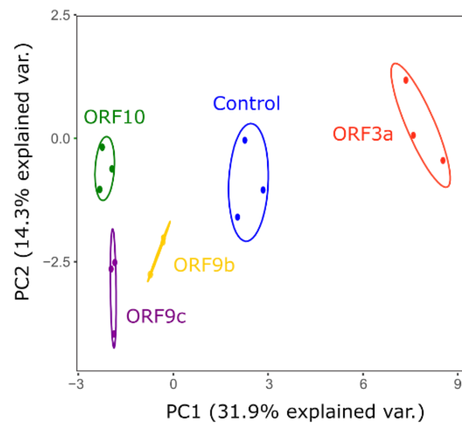

Figure S2. Principal Component Analysis (PCA) graph of A549 control cells and A549 cells transduced with ORF3a, ORF9b, ORF9c or ORF10 accessory proteins.

Supplementary Figure 3

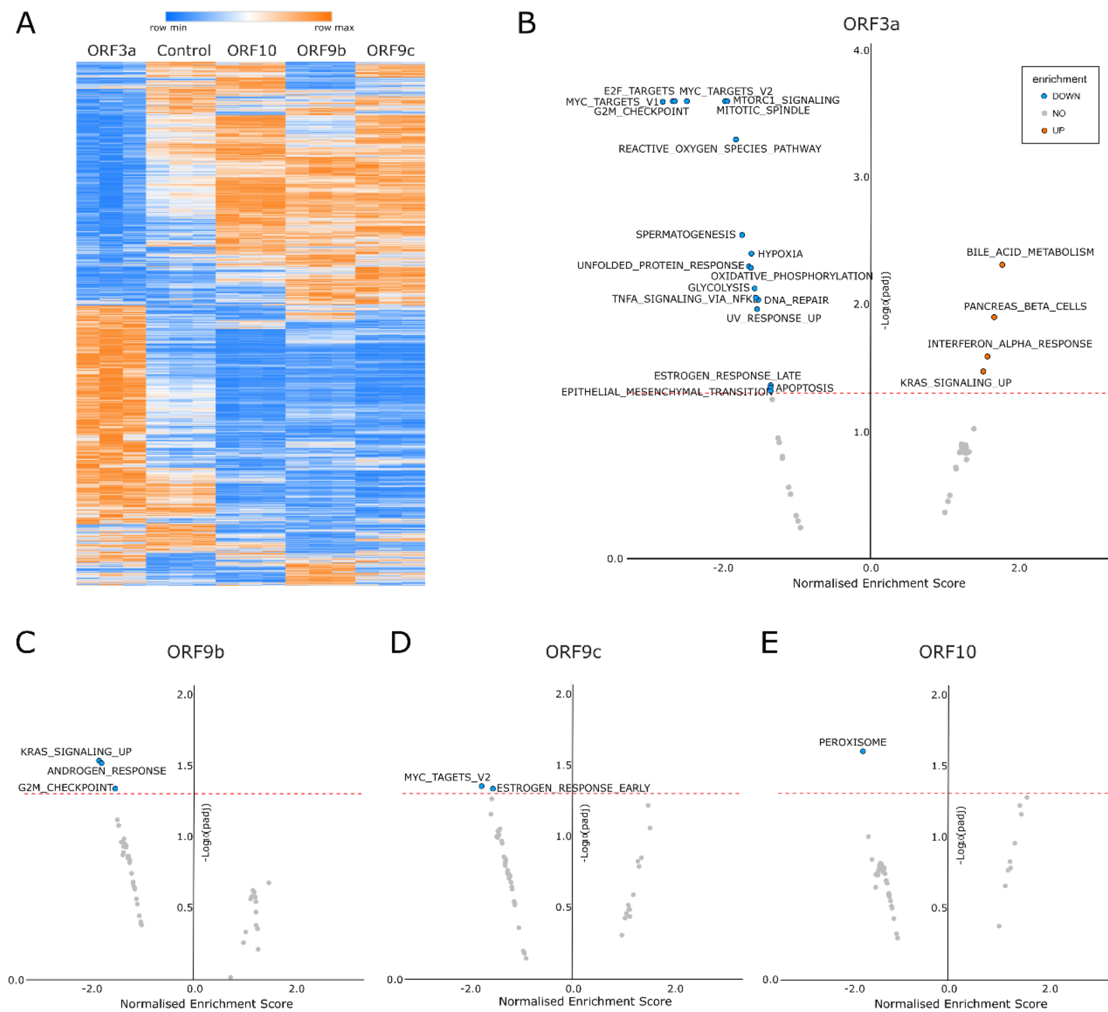

Figure S3. **(A)** Heatmap of RNA-Seq analysis of A549 control cells and A549 cells transduced with ORF3a, ORF9b, ORF9c or ORF10. **(B-E)** Volcano plots of enrichment scores for metabolic pathways, inferred after GeneSet Enrichment Analysis (GSEA) of differentially-expressed genes for ORF3a-A549 **(B)**, ORF9b-A549 **(C)**, ORF9c-A549 **(D)**, and ORF10-A549 cells **(E)**. Horizontal dashed red line represents -log10(padj) = 1.3 (p-value = 0.05).

Supplementary Figure 4

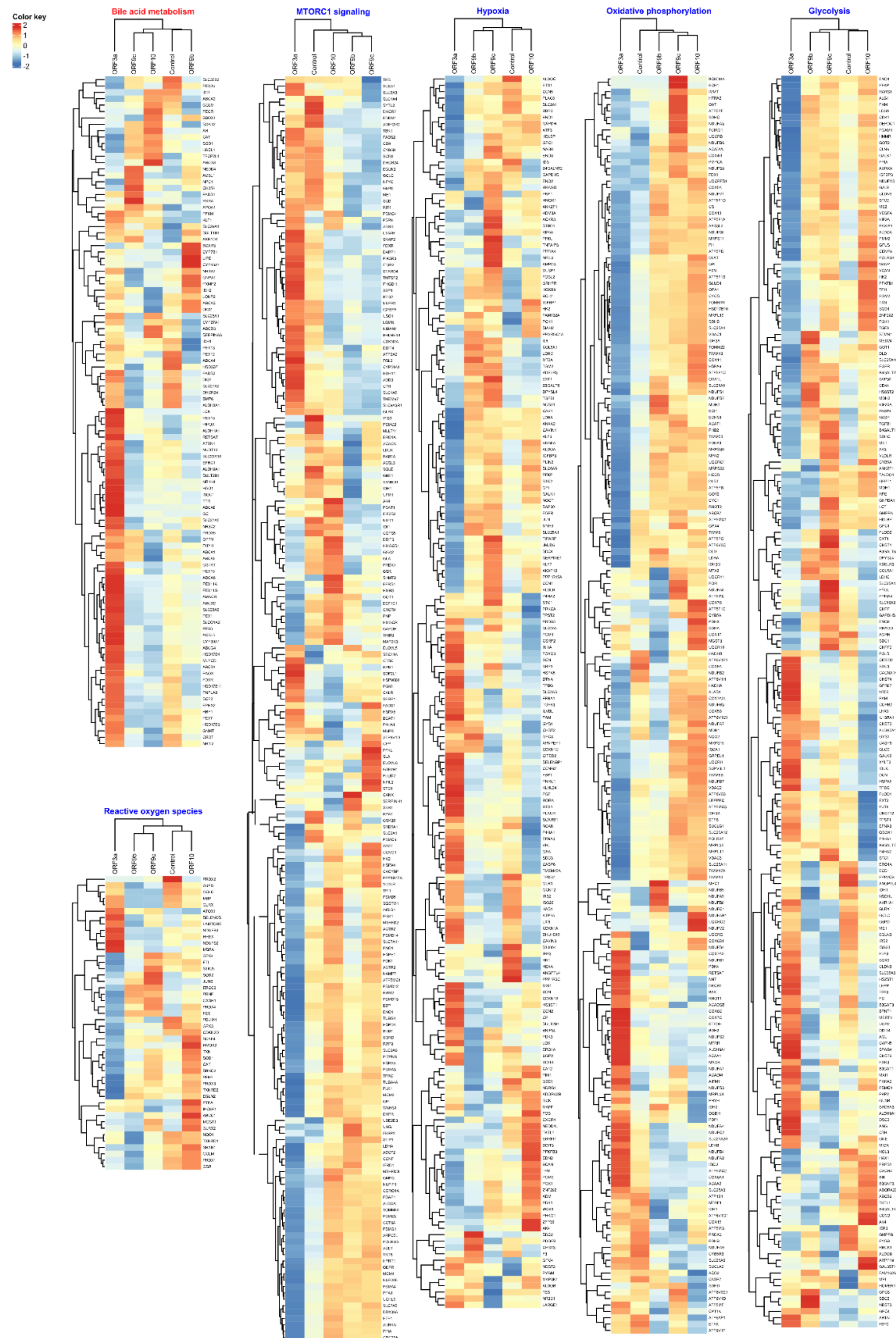

Figure S4. Extended heatmap of metabolic enrichment pathways altered by ORF3a expression represented in Fig. 2A. Gene expression pattern of each pathway in all A549 transduced cells

and A549 control cells was compared. The color key corresponds to row-normalized counts by variance stabilizing transformation (vst).

Supplementary Figure 5

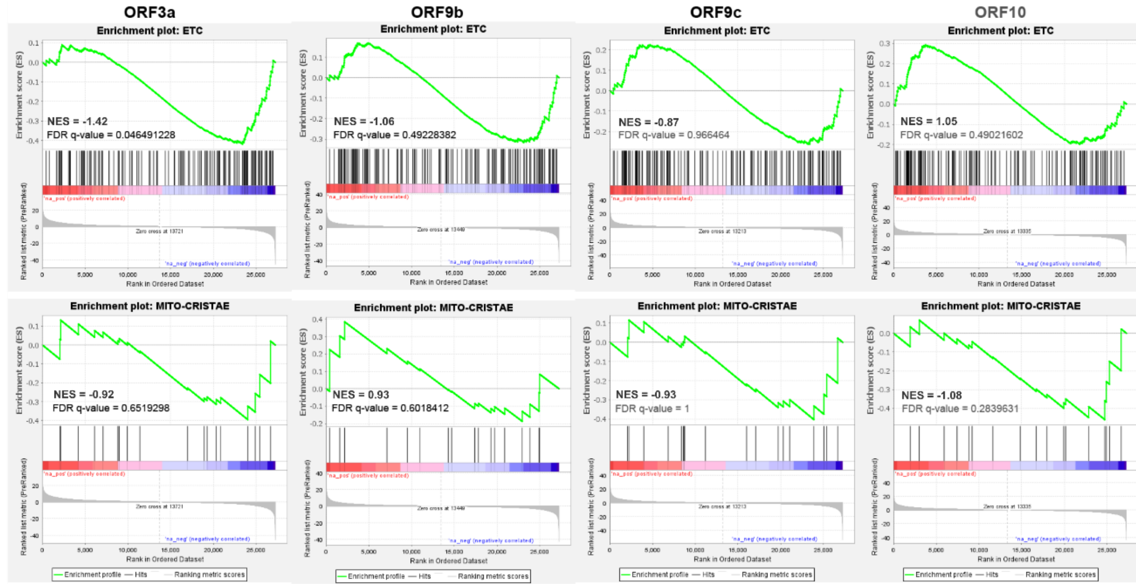

Figure S4. Enrichment plots of GeneSet Enrichment Analysis (GSEA) analysis for ETC and mitochondrial cristae gene sets.

Supplementary Figure 6

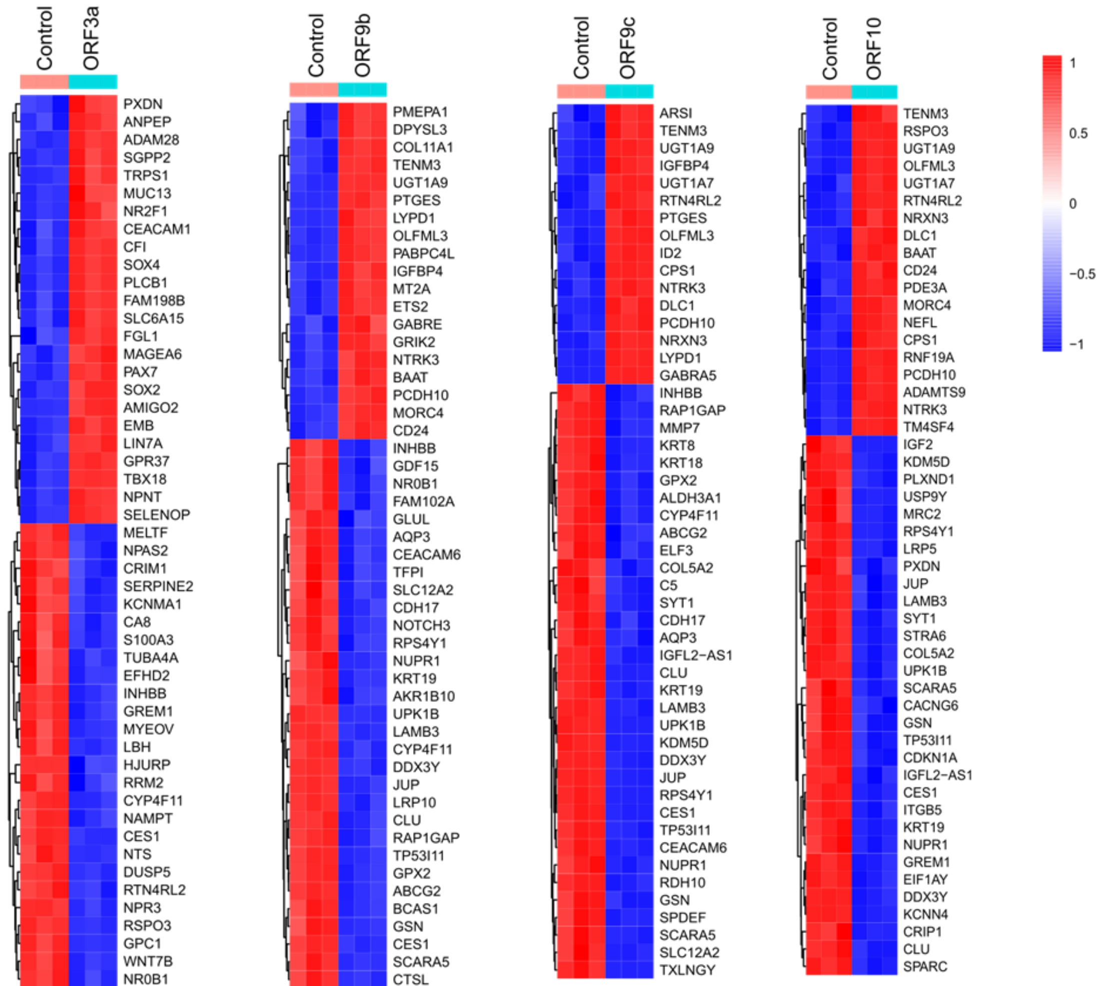

Figure S6. Heatmap of top 50 differentially expressed genes (DEGs), selected as significant DEGs ($p \leq 0.05$) with the highest and lowest Log_2FC values, induced by ORF3a, ORF9b, ORF9c and ORF10 in A549 cells, in individual comparisons of cells expressing each accessory protein with control cells. The color key corresponds to row-normalized values.

Supplementary Figure 7

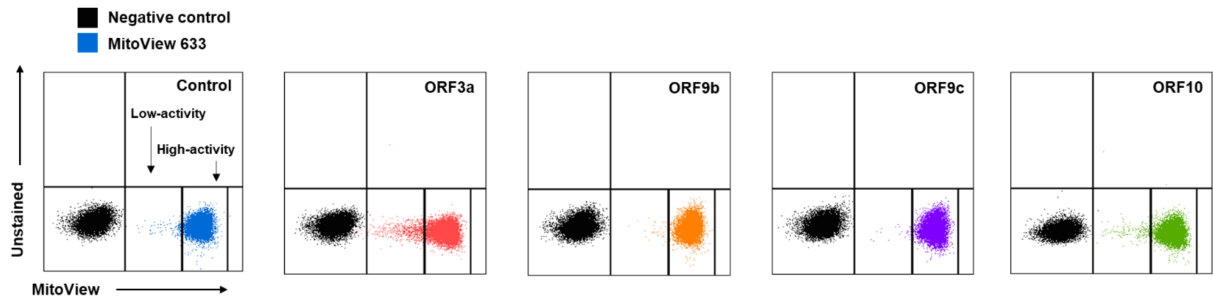

Figure S7. Analysis by flow cytometry of mitochondrial activity in ORF-A549 cells. Dotplot of control cells and A549 cells expressing ORF3a, ORF9b, ORF9c or ORF10. Cells were stained with MitoView 633 (5 nM) and showed two mitochondrial populations according to their activity: high-activity and low-activity mitochondria.

Supplementary Figure 8

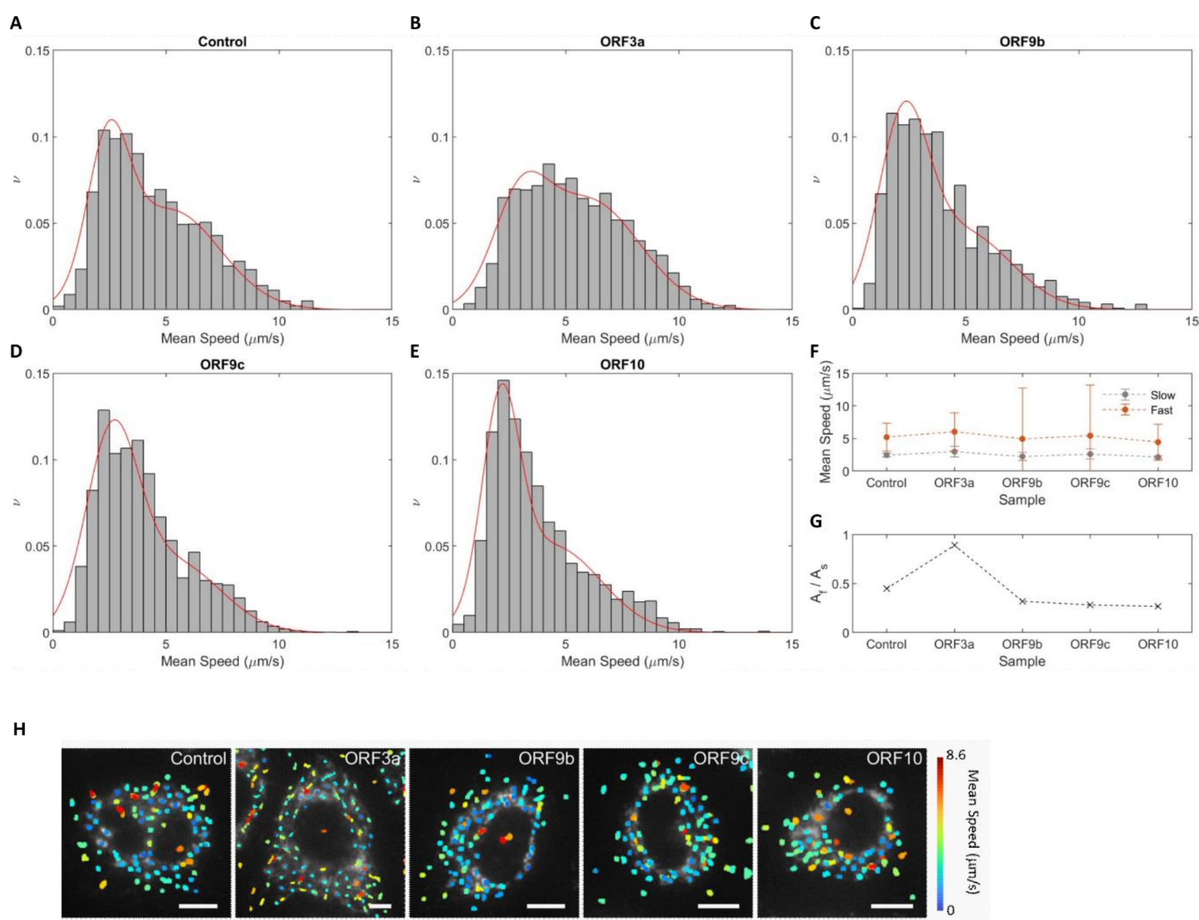

Figure S8. (A-E) Distributions of the mitochondria mean speed for each cell line. Bin counts are reported as relative frequencies in the Y axis (ν), i.e., the number of elements in each bin relative to the total number of elements in the input data. The red lines in the histograms represent the results of a multiple Gaussian fitting. In all cases, we individuated two Gauss-distributed populations. **(F)** The plot of the fitted mean values of both populations (indicated as "slow" and "fast") for each cell line. The error bars represent the standard deviations of the Gaussian fitting. **(G)** Ratio between the calculated areas under the Gaussians corresponding to the fast (Af) and slow (As) populations. **(H)** Representative results of the tracking performed on fluorescently labeled mitochondria. Taking the irregular shape of mitochondria into account, a mask-based segmentation to separate the different organelles was used. Track colors represent the average speed measured in between two frames. Scale bars: 10 μm.

Supplementary Figure 9

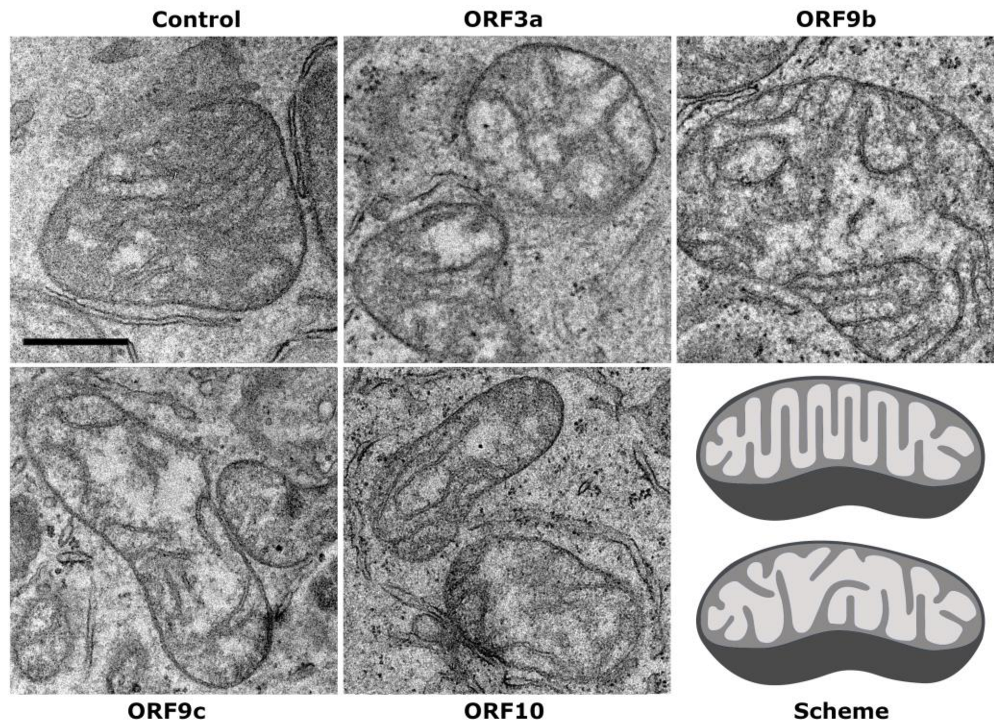

Figure S9. Mitochondrial morphology in ORF-A549 cells. Analysis by transmission electron microscopy of mitochondrial appearance in ORF-A549 cells ultrathin sections. Representative images of mitochondria in each condition. Scale bar indicates 500 nm. Last panel shows a schematic representation of mitochondria with organized and parallel mitochondrial ridges (top), and mitochondria with disorganized, non-parallel mitochondrial ridges and hollowed out areas (bottom).

Supplementary Figure 10

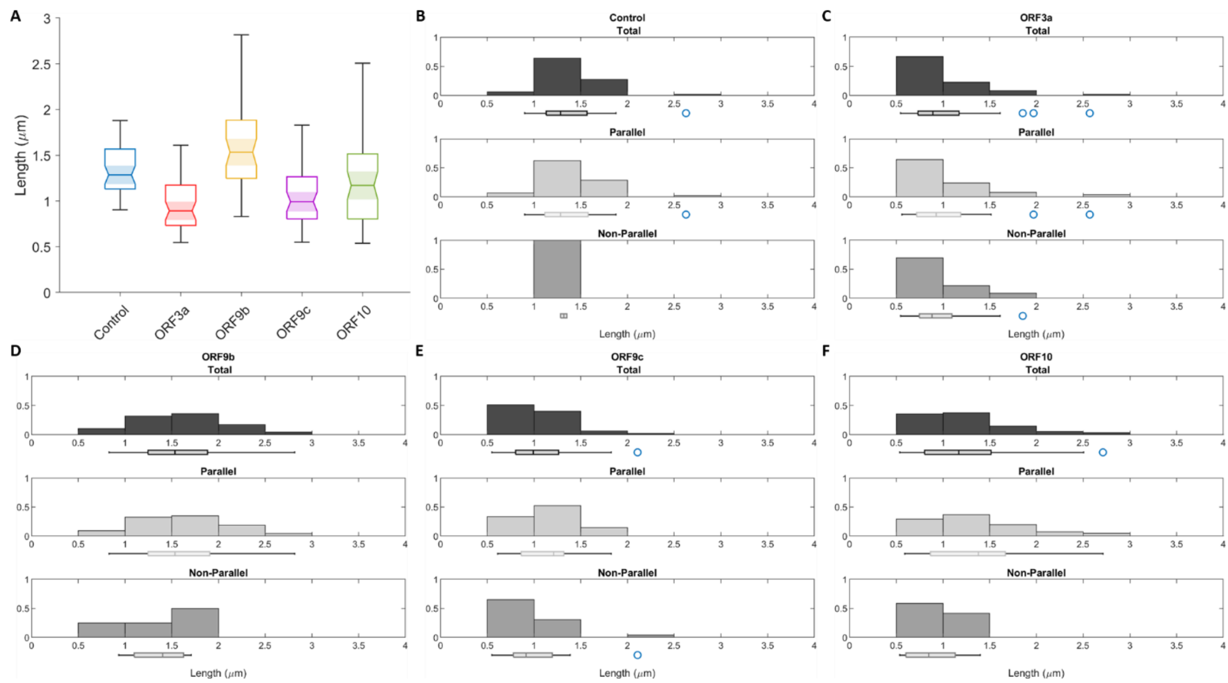

Figure S10. Distribution of the length of mitochondria in ORF-A549 cells imaged by transmission electron microscopy. **(A)** Box chart summarizing the distribution of the mitochondrial length measured in each cell line. Each box is divided into four sections representing a different quartile while the central lines are the median values and the areas marked in solid colors are the intervals of significance. The full distributions have been depicted in the histograms in **(B-F)**. For each cell line, the corresponding distribution of lengths has been plotted considering the total amount of measurements (upper histograms), as well as separating the mitochondria showing only parallel ridges from the mitochondria with non-parallel ones (middle and lower histograms).

Supplementary Figure 11

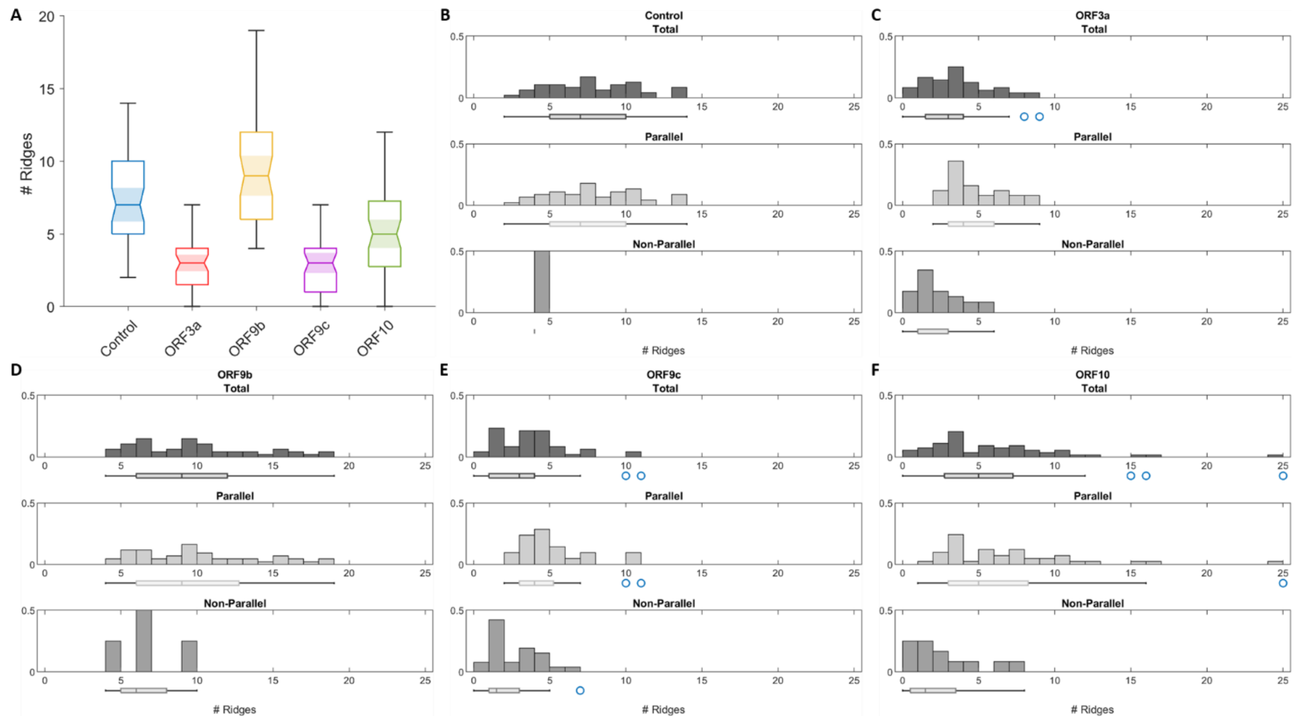

Figure S11. Distribution of the number of ridges per mitochondrion evaluated in ORF-A549 cells imaged by transmission electron microscopy. **(A)** Box chart summarizing the distribution of the number of ridges per mitochondrion counted for each cell line. Each box is divided into four sections representing a different quartile while the central lines are the median values and the areas marked in solid colors are the intervals of significance. The full distributions have been depicted in the histograms in **(B-F)**. For each cell line, the corresponding distribution of the number of ridges has been plotted considering the total amount of measurements (upper histograms) as well as separating the mitochondria showing only parallel ridges from the mitochondria with non-parallel ones (middle and lower histograms).